

## The strain-rate effects on the numerical simulation of steel beams under blast loads

S. K. Hashemi & M. A. Bradford

*Centre for Infrastructure Engineering and Safety,  
School of Civil and Environmental Engineering,  
The University of New South Wales, Australia*

### Abstract

Currently, there is significant interest amongst computational mechanics researchers in the area of investigating structures under blast loads. The explosive effect can impart damage, ranging from minor to full structural failure. Recent advancements in computer technology have enabled the ability to implement software in an efficient and cost-effective way to model complicated blast scenarios. To achieve better agreement between numerical and experimental models, the behaviour of the materials must be defined precisely and correctly. Dynamic loads are much more complicated than static loads, and so all parameters which could possibly affect the results and their further interpretation should be assigned carefully. Therefore, different values for  $C$  and  $P$  – as Cowper-Symonds strain-rate coefficients in LS DYNA – are considered in a simulation of  $W150 \times 24$  steel beams under two different blast shots, and are compared with experimental results to determine strain-rate effects. To distinguish between different models, an error analysis is used based on scaling the absolute differences between the exact and derived results with the application of exponential and linear utility functions for four different performance criteria. The results show that the strain-rate effect must be taken into account in models containing blast loads, even when the strain rates experienced are relatively small. Moreover, the maximum deflections along the beam length show less dependency, while the residual deflections and maximum strain depend significantly, on the strain rate. The best model with less average error is derived when  $C$  and  $P$  equal  $20 \text{ s}^{-1}$  and 7, respectively.

*Keywords:* numerical, blast, steel beam, strain rate, LS-DYNA.



# 1 Introduction

There is significant interest amongst computational mechanics researchers in the area of investigating structures under blast loads. The explosive effect can impart damage, ranging from minor to full structural failure. Numerical techniques can be used to model the explosion and structure, so as to study the interaction between them. Recent advancements in computer technology have enabled the ability to implement software in a viable, efficient and cost-effective way to model complicated blast scenarios (Hashemi [1]). To achieve better agreement between numerical and experimental models, the behaviour of the materials must be defined precisely and correctly. Dynamic loads are much more complicated than static loads, and hence all the parameters which could possibly affect the results and their further interpretation should be assigned carefully (Bischoff and Perry [2]). The strengths and dynamic mechanical properties of the materials can be enhanced significantly to high strain rates which can range from  $0.01$  to  $1000 \text{ s}^{-1}$  due to blast loads. Fig. 1 shows the magnitudes of strain rates expected for different load types.

The main objective of this investigation is to evaluate the strain-rate effects on a simulation undertaken of  $W150 \times 24$  steel beams under blast loads using LS DYNA. Different values for the Cowper-Symonds (CS) strain-rate coefficients  $C$  and  $P$  are set in the models and investigated to achieve the best agreement with experimental results. To distinguish between different models, a special error analysis is used based on scaling the absolute differences between the exact and derived results with an application of exponential and linear utility functions for four different performance criteria.

Different methods have been used to determine the strain-rate behaviour of materials experimentally such as the quasi-static tension test, the Split Hopkinson Pressure Bar and the Taylor impact test, and many researchers have used computational methods to model strain hardening in order to determine the material parameters for the material definition. This concept has been challenged by Allen *et al.* [3], who used a numerical approach to refine the material constants by reducing the difference between the results of a series of Taylor tests and simulations at different impact velocities.

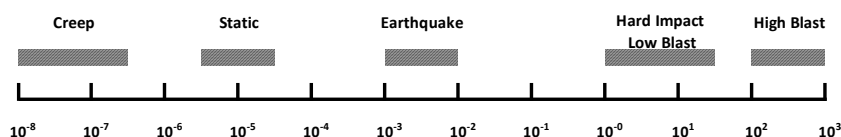


Figure 1: Magnitude of strain rate expected for different load cases [2].

Sasso *et al.* [4] used a finite element modelling of Split Hopkinson Pressure Bar tests on steel to adjust the material behaviour, while Milani *et al.* [5] proposed a strategy for obtaining the material parameters for the Johnson-Cook

constitutive model. They compared the results from models with Split Hopkinson Pressure Bar tests at different strain rates and temperatures and refined the parameters by an application of optimisation. Hernandez *et al.* [6] developed a technique for the dynamic characterization of metals based on the formulation and solution of a first-class inverse problem. The characterisation procedure consists of the determination of the CS material model constants from a single Taylor impact test, in the order of  $10^4 \text{ s}^{-1}$  to  $10^6 \text{ s}^{-1}$ . The numerical models showed that the procedure is capable of capturing the shape of the Taylor test specimen with an error of less than 10%.

In the current paper, optimisation of the models is based on reducing the scaled absolute differences between the exact and derived results in four specific criteria. These criteria are maximum and residual deflections, as well as the maximum and minimum strains along the beam length. A scaling method is considered with the application of exponential and linear utility functions.

## 2 Method of analysis

The effect of the strain rate on the numerical modelling of a  $W150 \times 24$  steel beam is investigated using LS-DYNA [7]. This section is widely used in steel frame structures with a nominal static yield stress and ultimate strength of 393 MPa and 537 MPa respectively. The span length is 2.41 m, and the beams were subjected to two blast scenarios generated by different stand-off distances. In the first shot, 50 kg of ANFO is placed at distance of 10.3 m from the face of the flange of the beam while in the second shot, the distance is decreased to 7 m and the explosive mass is increased to 250 kg of ANFO. The beams are modelled as being simply supported vertically, which is the same as the tests with the self-weight along the beam included. Table 1 indicates the different test setups. Each beam was modelled with quadrilateral, four-node fully integrated shell elements because they provide accurate results and require a relatively small amount of computation time. An attempt is made to keep the mesh sizes around 5 mm with an aspect ratio of around unity for better results. A mesh sensitivity analysis has been carried with mesh sizes of 3 mm, 10 mm and 20 mm.

LS-DYNA [7] is a general-purpose finite element program capable of simulating complex explosion-structure interactions. A typical view of the FE model is shown in Fig. 2. To define the steel material, an elasto-plastic material with strain-rate dependency, MAT\_PIECEWISE\_LINEAR\_PLASTICITY, was used. Table 2 shows the parameters used to model the steel materials. Two parameters,  $C$  and  $P$ , which are related to the CS equation, need to be adjusted carefully to simulate the effect of strain rate in the model.

The CS equation has been used extensively in situations where an estimate of the increase of the flow stress due to material strain-rate sensitivity is necessary. The CS material model is a simple elasto-plastic, strain-rate hardening model that uses an empirical formulation, in which the materials strengthen when plastic deformations are applied. This behaviour is known as strain hardening. The CS material model scales the initial yield stress ( $\sigma_y$ ) by two factors: a strain factor and a strain-rate factor as given by (Cowper and Symonds [8]):

$$\frac{\sigma_y}{\sigma_0} = 1 + \left( \frac{\dot{\epsilon}}{C} \right)^{1/P}, \quad (1)$$

where  $\sigma_0$  is the static yield stress,  $\dot{\epsilon}$  is the strain rate and  $C$  and  $P$  are the CS strain-rate parameters. The CS parameters have to be determined from experimental observations and as a consequence, the performance of the material model relies on experimental data from which the parameters have been fitted. The ability to accurately describe the material behaviour is shared jointly between the strength model selection and the values of the associated constants [8]. The implementation of this material model is linked with the determination of the values for  $C$  and  $P$ , and so different values are chosen for  $C$  and  $P$ ; the values for  $C$  range from  $10 \text{ s}^{-1}$  to  $500 \text{ s}^{-1}$  and the values for  $P$  range from 2 to 9.

Table 1: Test setup.

Shot	Charge ANFO (kg)	Equiv. TNT (kg)	TNT/ANFO mass ratio	Stand-off (m)	Scaled dist. (m/kg <sup>1/3</sup> )
1	50	42	0.84	10.3	2.96
2	250	210	0.84	7.0	1.18

Table 2: Material parameters for steel.

Density, $\rho$ (kg/m <sup>3</sup> )	Elastic modulus (GPa)	Yield stress (MPa)	Tang. modulus (MPa)	Poisson's ratio
7850	210	400	540	0.25

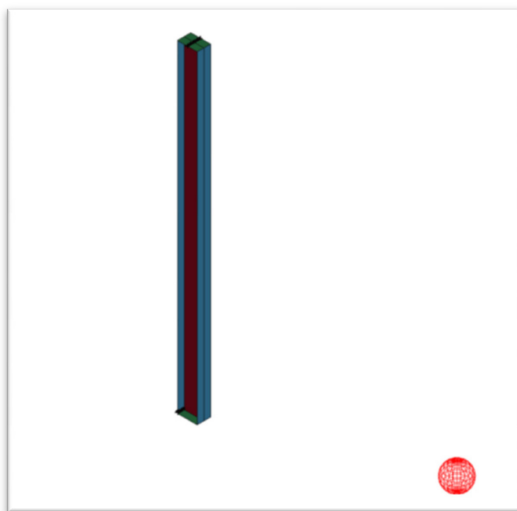


Figure 2: Typical FE modelling.

To apply blast loading, the input key `LOAD_BLAST_ENHANCED` was used. This feature includes enhancements for treating reflected waves, moving warheads and multiple blast sources. The loads are applied to facets defined with the keyword `LOAD_BLAST_SEGMENT_SET`. When a charge is located on or very near the ground surface it is considered to be a surface burst. In this circumstance, the initial blast wave is immediately reflected and reinforced by the nearly un-yielded ground to produce a reflected hemispherical wave that moves out from the point of the burst. This reflected wave merges with the initial incident wave to produce overpressures which are greater than those produced by the initial wave alone. By choosing `BLAST = 1`, hemispherical surface burst, this effect is taken account of in the model [7]. This option applies a pressure history that models a Mach front from the interaction of the incident waves from the initial blast and the reflected waves off the ground. The air burst strengthened by the ground reflection option is an acceptable replacement for an ALE analysis.

The keyword `DATABASE_BINARY_D3PLOT` is used to indicate how often the results should be saved in the results file. While larger values for `DT` may cause missing intermediate results, a value of  $50\ \mu\text{s}$  is determined to have small variations (less than 2%) in capturing the data of interest between the time steps. The keyword `CONTROL_TERMINATION` is used to dictate when the analysis should end. A termination time of 30 ms was typically used in the models.

### 3 Validation study

Experimental tests using live explosive charges on the member types under consideration in this study have been carried by Nassr *et al.* [9]. The results are used to validate the modelling methods described above and different sets of strain-rate constants parameters. A TNT equivalent mass was used instead of ANFO, even though the latter was used in each blast shot in the referenced work. To ensure adequate explosive mass was used in the simulation, the reflected pressure and impulse were checked to be the same as that derived from the experimental tests. Fig. 3 demonstrates the adequacy of predicted reflected pressure and impulse at different point.

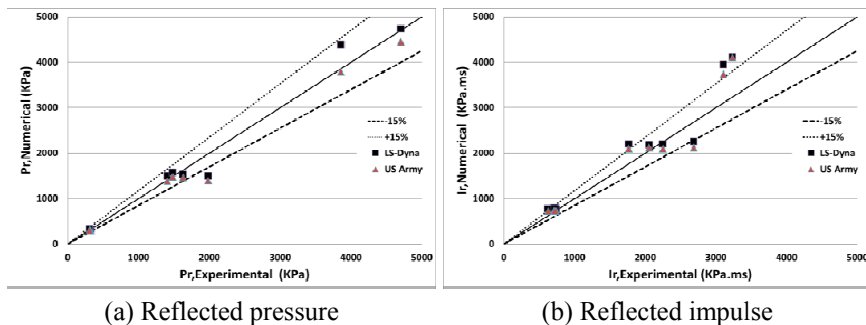


Figure 3: Comparison of reflected pressure and reflected impulse.

# 4 Results

To distinguish between different models with different  $C$  and  $P$  strain-rate coefficients, an error analysis has been undertaken based on scaling or mapping the absolute differences between the exact and derived results in the range of 1 to 10 by applying exponential and linear utility functions separately. The exponential utility function has mostly been used in multi-attribute decision analysis and can apply weights to different ranges of errors. A score of 10 means that the derived result is exactly the same as the experimental result. As noted, four series of criteria have been chosen, *viz.* the maximum and residual deflections along the beam height as well as the maximum and minimum strains at mid-span, one-third and one-sixth of beam length lower part. The average scores for these criteria were calculated and compared to derive the model which represents the experimental test best. The exponential utility function

$$F(x) = 1 + Ae^{-Bx} \tag{2}$$

was used in this study, for which the best returned score is 10 and the worst is 1. To do so, the coefficient  $A$  is equal to 9. The coefficient  $B$  was calculated based on two concepts; firstly that the function must return unity when the worst result is taken, and secondly and which is an assumption, those results within 20% of the difference between the exact and worst results in any criteria should return a value larger than 4.5. A sensitivity calculation has been undertaken to understand the effect of chosen values in the range 3 to 5. These showed that with any assumed value between 3 and 5, the best three models are the same. Many other utility functions can clearly be used to evaluate the results, and so a linear utility function has been used and the results provided to compare the two methods. For this, the exact and worst results are interpolated linearly between 10 and 1.

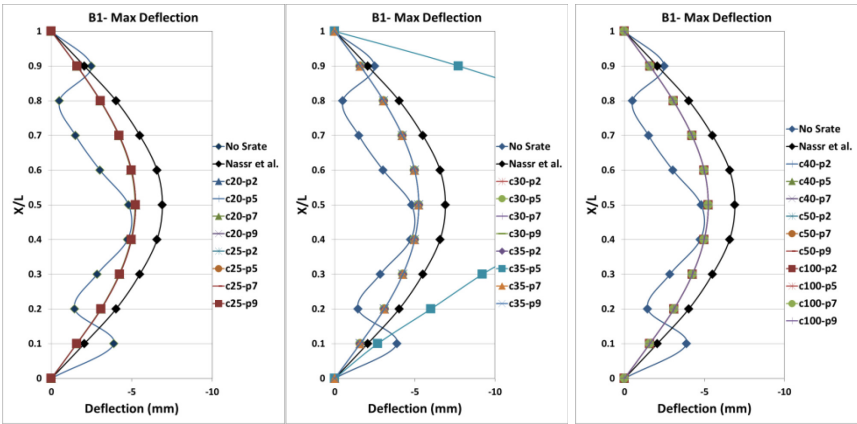


Figure 4: Maximum deflection along beam length for shot 1.



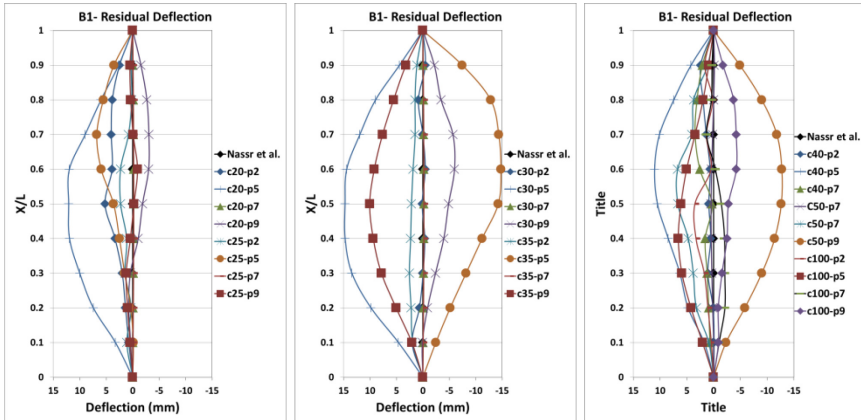


Figure 5: Residual deflection along beam length for shot 1.

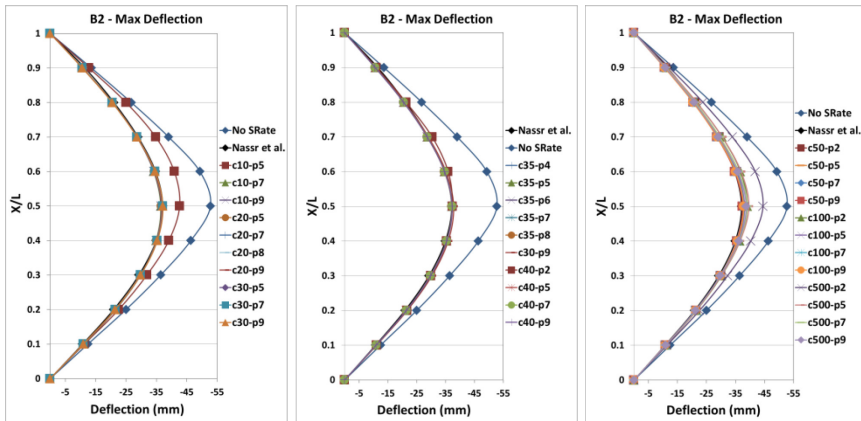


Figure 6: Maximum deflection along beam length for shot 2.

More than 200 numerical models were assembled and investigated, and although all of the results were used to determine the best models, a selection of the results is presented here in the form of graphs and tables. Figs. 4 to 7 show the maximum and residual deflections along the beams with different models. Shot 2 results in more deflections with zero strain rate, but zero strain rate for shot 1 does not produce any significant deformations. It can be seen from the figures that the residual deflections are quite dependent on the strain rate defined by the coefficients  $C$  and  $P$ , while the maximum deflections are much less sensitive.

Tables 3 and 4 provide details of the maximum deflections, strain and strain rate plus calculated scores for a selection of the models. As for the residual deformations, the maximum and minimum strains depend significantly on strain-rate parameters.

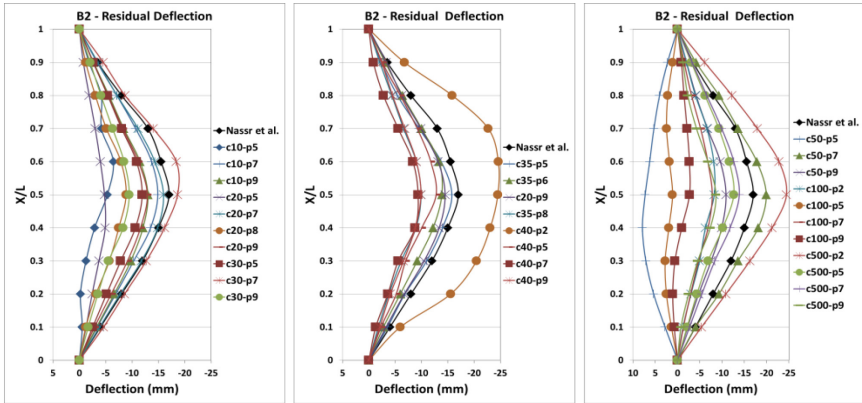
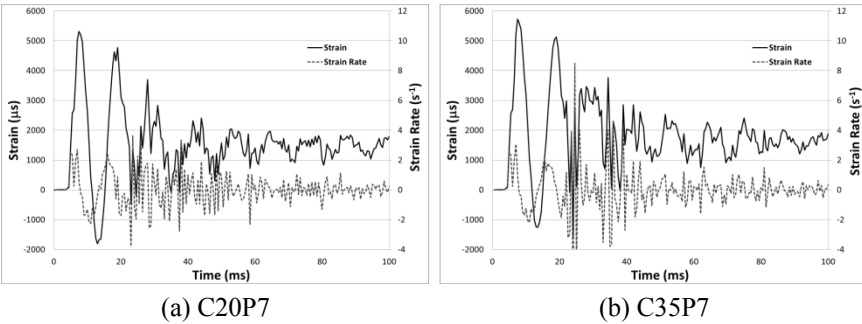


Figure 7: Residual deflection along beam length for shot 2.



(a) C20P7 (b) C35P7

Figure 8: Strain and strain-rate time history at mid-span for shot 2.

For shot 1, the error scaling analysis has shown the model with  $C = 20 \text{ s}^{-1}$  and  $P = 7$  has less cumulative error (comparing the fourth decimals). With very small differences, the models with  $C = 25, 30$  and  $35 \text{ s}^{-1}$  and  $P = 7$  produces less than 0.2% error regarding the best model. Taking account of the absolute average percentage error calculated based on the maximum deflection and maximum strain at mid-span has shown an error of around 15% in comparison with the experimental results.

The best model achieved scores of 6.21 and 7.94 with an application of exponential and linear utility functions respectively. It must be noted that when the best models achieve a score of 6.21, it shows the distance between the worst results and the exact value are much less and with the assumption to scale the errors with the exponential utility function, the differences between results obtained in the best models and exact values are less than 20% of difference between exact and worst results obtained in all range of the models. Moreover, the exponential error scaling showed almost 60% of models had scores larger than 5.28 (85% of best score). This means beam in shot 1 has less sensitivity to strain rate.





Table 3: Error analysis for shot 1.

Model No.	Model Name	MaxDeflection		ResidualDeflection		Maxstrain	Strain Rate	Scores (max=10)										Percentage Error
		mm		mm				Exp. Function		Lin. Function		Exp. Function		Lin. Function		Exp. Function		
		mm	mm	mm	mm	μs		s <sup>-1</sup>	Max & ResidualDeflection	Max & ResidualDeflection	Max & ResidualDeflection	Max & ResidualDeflection	Max & Mm Strain	Max & Mm Strain	All Criteria	All Criteria	Absolute Average*	
00	Experimental	-6.90	0.00	0.00	0.00	559.0	0.28	10.00	10.00	10.00	10.00	10.00	10.00	10.00	10.00	10.00	0.00	
19	B1-c40-p7	-5.24	0.29	0.13	0.29	593.5	0.37	6.47	9.00	4.31	6.20	4.31	6.20	5.390	7.60	7.60	15.14	
38	B1-c30-p2	-5.20	0.13	0.13	0.13	589.4	0.34	7.56	9.33	4.46	6.46	4.46	6.46	6.010	7.89	7.89	15.04	
43	B1-c20-p7	-5.20	-0.19	-0.19	-0.19	588.8	0.34	7.96	9.42	4.47	6.45	4.47	6.45	6.212	7.94	7.94	14.99	
44	B1-c25-p7	-5.20	-0.19	-0.19	-0.19	588.8	0.34	7.96	9.42	4.47	6.45	4.47	6.45	6.211	7.94	7.94	14.99	
45	B1-c30-p7	-5.20	-0.19	-0.19	-0.19	588.8	0.34	7.96	9.42	4.47	6.45	4.47	6.45	6.212	7.94	7.94	14.99	
46	B1-c35-p7	-5.20	-0.19	-0.19	-0.19	588.7	0.34	7.96	9.42	4.47	6.45	4.47	6.45	6.212	7.94	7.94	14.98	
48	B1-C50-p7	-5.20	0.48	0.48	0.48	588.7	0.34	7.85	9.40	4.47	6.45	4.47	6.45	6.156	7.93	7.93	14.99	

\* Absolute average percentage error calculated based only on Max Deflection and Max strain

Table 4: Error analysis for shot 2.

Model No.	Model Name	Max Deflection		Residual Deflection		Max strain	Strain Rate $s^{-1}$	Scores (max=10)										Percentage Error
		mm	mm	mm	mm			Exp. Function		Lin. Function		Exp. Function		Lin. Function		All Criteria		
						Max		Deflection	Max	Deflection	Exp. Function	Lin. Function	Exp. Function	Lin. Function				
															Max & Residual Deflection		Max & Min Strain	
00	Experimental	-37.06	-17.00	3610	2.89		10.00	10.00	10.00	10.00	10.00	10.00	10.00	10.00	10.00	0.00		
4	B2-c10-p9	-36.54	-13.00	5035	10.89		8.53	9.65	8.78	9.72	8.65	9.68	8.65	9.68	9.68	21.47		
14	B2-c40-p5	-37.26	-12.78	13961	29.32		8.37	9.59	5.97	8.71	7.17	9.15	7.17	9.15	104.04	104.04		
15	B2-c40-p7	-37.27	-9.36	5775	10.29		7.67	9.36	8.01	9.51	7.84	9.44	7.84	9.44	35.17	35.17		
30	B2-c35-p6	-37.16	-13.86	5599	3.55		8.74	9.71	8.37	9.62	8.56	9.66	8.56	9.66	24.61	24.61		
40	B2-c20-p7	-37.45	-15.96	5310	3.64		9.24	9.83	8.50	9.65	8.87	9.74	8.87	9.74	18.09	18.09		
46	B2-c35-p7	-37.84	-15.18	5730	8.49		8.78	9.71	8.45	9.64	8.61	9.68	8.61	9.68	23.85	23.85		
57	B2-c20-p9	-37.55	-14.49	5665	8.11		8.80	9.72	8.32	9.61	8.56	9.66	8.56	9.66	24.33	24.33		

\*\* Absolute average percentage error calculated based only on Max and Residual Deflection and Max strain



Similarly for shot 2, the model with  $C = 20 \text{ s}^{-1}$  and  $P = 7$  has less cumulative error. With very small differences, the models with  $C = 10 \text{ s}^{-1}$  and  $P = 9$  and  $C = 35 \text{ s}^{-1}$  and  $P = 7$  produce more accurate results. The absolute average percentage error calculated based on the maximum and residual deflections and the maximum strain at mid-span shows an error of around 18% compared with the exact values. The scores for the best model are 8.87 and 9.74 with application of the exponential and linear utility functions, respectively. Hence, some models in shot 2 produced results which are far from accurate values because the scores for the best models are much closer to 10. Additionally, the exponential error scaling showed only around 45% of the models had scores larger than 7.54 (85% of the best score). Unlike shot 1, the strain rate has more effect on the beams in shot 2.

Fig. 8 shows the strain and strain-rate time history at mid-span for shot 2, with more results being provided in Tables 3 and 4. From the figure, it is clear that considering the strain-rate effect in models by defining the CS coefficients results in a better deflection trend for both shots. Although the residual deflections depend significantly on the strain rate, the maximum deflections show less dependency. This dependency in shot 1 is almost zero and in shot 2, the maximum deflections are mostly within a tolerance of  $\pm 2\%$ . The residual deflections can be predicted with adequate strain-rate parameters. Some models show maximum residual deflections less than 0.2 mm (versus no residual deflections in the experiments) for shot 1 and around 16 mm (versus 17 mm experimental) permanent deflection at mid-span for shot 2.

## 5 Conclusions

The main objective of this investigation has been to investigate strain-rate effects on the simulation of  $W150 \times 24$  steel beams under blast loads, using LS-DYNA. Different values for the Cowper-Symonds strain-rate coefficients –  $C$  and  $P$  – were set in the numerical models, and investigated to achieve the best agreement with experimental results. To distinguish between the different models, an error analysis has been used based on scaling the absolute differences between exact and derived results within a range of 1 to 10 with the application of exponential and linear utility functions in four different criteria.

The results of the different models indicate that:

- The strain-rate effect must be taken into account in models that treat blast loads, even if the strain rate is relatively small. Failure to consider the strain rate will lead to overestimated deflections and strains.
- The maximum deflections along the beam length are less dependent on the strain rate, while the residual deflections and maximum strain depend significantly on the strain rate.
- Models with smaller strain rates are less dependent on the Cowper-Symonds coefficients and so a wider range of values can be used.
- For the case treated, models with  $C = 20 \text{ s}^{-1}$  and  $35 \text{ s}^{-1}$  and  $P = 7$  provided solutions that agreed well with the test results. In this case, the strain rate was in the order of  $10^{-1}$  to  $10^0 \text{ s}^{-1}$ .



## References

- [1] Hashemi, S.K. & Bradford, M.A., Numerical simulation of free-air explosion using LS-DYNA. *1<sup>st</sup> Australasian Conference on Computational Mechanics*, Sydney, 2013.
- [2] Bischoff, P.H. & Perry, S.H., Compressive behaviour of concrete at high strain rates. *Materials and Structures*, **24**, pp. 425-450, 1991.
- [3] Allen, D., Rule W. & Jones, S., Optimizing material strength constants numerically extracted from Taylor impact data. *Experimental Mechanics*, **37**, pp. 333-338, 1997.
- [4] Sasso, M., Newaz, G. & Amodio, D., Material characterization at high strain rate by Hopkinson Bar tests and finite element optimization. *Materials Science and Engineering A*, **487**, pp. 289-300, 2008.
- [5] Milani, A., Dabboussi, W., Nemes, J. & Abeyaratne, R., An improved multi-objective identification of Johnson–Cook material parameters. *International Journal of Impact Engineering*, **36(2)**, pp. 294-302, 2009.
- [6] Hernandez, C., Maranon, A., Ashcroft, I.A., Casas-Rodriguez, J.P., A computational determination of the Cowper–Symonds parameters from a single Taylor test. *Applied Mathematical Modelling*, **37(7)**, pp. 4698-4708, 2013.
- [7] Hallquist, J.O., *LS-DYNA Theory Manual*, Livermore Software Technology Corp., Livermore, California, 2006.
- [8] Cowper, G., & Symonds P., Strain hardening and strain-rate effects in the impact loading of cantilever beams. Technical Report, Brown University Division of Applied Mathematics, Providence, Rhode Island, 1957.
- [9] Nassr, A., Razaqpur, A., Tait, M., Campidelli, M. & Foo, S., Experimental performance of steel beams under blast loading. *Journal of Performance of Constructed Facilities*, *ASCE*, **26(5)**, pp. 600-629, 2012.

